UNIT-IV:
WIND ENERGY SYSTEMS:

Generation schemes with variable speed turbines: classification of schemes – operating area – Induction Generators-Doubly fed Induction generators-Equivalent circuits-Reactive power and harmonics-Double output system with VSI-Variable voltage, variable frequency generation-circuit model and steady state operation and characteristics- effect of wind generator on the network. Wind speed measurements-Wind speed statistics-site and turbine selection.

4.1 Generation schemes with variable speed turbines:

4.1.1 classification of schemes

Broadly, four different systems are used for generation of electricity from wind power.

4.1.1.1 Constant-speed, constant-frequency

The generation scheme in this category is based on fixed-speed technology. The horizontal-axis wind turbine, whose speed can be controlled by using a pitch-control mechanism, operates at a constant speed and drives, through a gear box, a synchronous or an induction generator that is connected to the power network.

A constant-speed wind turbine can achieve maximum efficiency at the speed that gives the tip speed ratio the value corresponding to the maximum power coefficient Cp Opt. Its main weakness lies in its poor energy capture from the available wind power at other wind speeds. Moreover, a pitch-control mechanism adds considerably to the cost of the machines and stresses the operating mechanism and the machines.

4.1.1.2 Near-constant-speed, constant-frequency

In this scheme, induction generators feed power to the utility network at variable slip. Here also the generators are driven by horizontal-axis wind turbines but with a less stringent pitch angle controller, which can maintain small values of slip.

4.1.1.3 Variable-speed, variable-frequency

This scheme employs capacitor self-excited three-phase or single phase induction generators for small-scale power generation as a source of isolated supply to feed frequency-insensitive loads.

4.1.1.4 Variable-speed, constant-frequency

Wind turbines are basically variable-speed prime movers. This category implies a wide and continuous range of variable-speed operation of the turbine and the processing of power ultimately at the synchronous frequency of the utility system. Variable-speed operation of wind turbines offers several benefits. So there is a general trend now towards generation schemes employing variable- speed turbines. There are many reasons for such a choice, which may be briefly summarized as follows.

(a) Continuous operation of wind turbines at the optimum tip speed to wind speed ratio by changing the rotor speed with the wind velocity. This increases energy capture even under low wind conditions.
(b) Reduction in noise emission from wind turbines at low wind speeds.
(c) Reduction in the size and weight of the gear box, or its total elimination, together with the associated noise
(d) The possibility of power smoothing due to the inertial energy storage in the turbine rotor as the wind gusts above the average level. With reduction in the wind speed, the power flow level in the network can be maintained by deriving additional energy from the inertia of the system. The time trace of the power output of a constant-speed wind turbine is characterized by high-frequency fluctuations superimposed on slow power variations owing to the short-term wind fluctuations and inherent time lag in the wind turbine control system. On the other hand, the time trace of the power output of a variable-speed system is considerably smoother due to the rotor flywheel effect.

The variable shaft speed leads to variable-voltage, variable frequency output from the generator, in general. However, in certain systems, the output voltage magnitude can be maintained constant, or within a range, by a voltage-regulating system.

The variable-voltage, variable-frequency system requires effi ancient power electronic ac/dc/ac converters for interfacing with the utility system. Converters using power electronic devices have good dynamic performance, and can provide high-quality sine wave current in the generator and the power network. They can also help to control the real as well as the reactive power of the system Furthermore, when a number of wind generators ope in parallel, the converters can optimize the output of each machine in order to increase the total power output, by allowing different machines to operate at different speeds.

4.1.2 Operating Area

Though maximum energy capture is an important factor in the variable-speed operation of wind turbines, in actual operation, limits on the shaft torque, power, and speed determine the overall control strategy. The operating area of a wind turbine is depicted in Fig. 6.1, showing the torque-speed characteristics with increasing wind velocity. AB, BD, and DE, respectively, define the limits of shaft torque, power, and speed. Within the area OABDE a number of control strategies can be adopted. The operating point in the torque-speed plane for variable-speed operation at maximum C, follows the square-law curve OC. At C, the power limit is reached, beyond which the turbine operates along CD, maintaining a constant power limit at reduced torque until the speed limit Q1Q2 is reached. Constant-speed operation along P P2 and Q1Q2 are limited by the maximum torque and maximum power, respectively. If the torque and the speed constitute the only turbine operation limits, OAZE would be the safe operating area of the turbine. This will allow an improvement in the energy capture up to W.

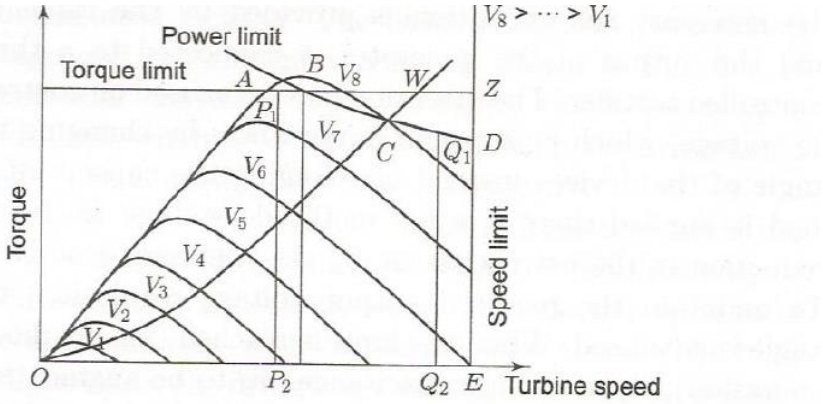

Wind turbine torque–speed characteristics at different wind speeds

4.2 Induction Generators

An induction machine in the generating mode operates fundamental tally in the same manner as in the motoring mode except for the reversal of power flow. Consequently, the equivalent circuit and the associated performance equations, derived earlier using motoring conventions, are valid for all values of slip. With the stator winding remaining connected to the utility grid, if the rotor is driven by a prime mover above the synchronous speed in the direction of the air-gap field, the mechanical power of the prime mover is converted into electrical power.

4.2.1 Cage Rotor Induction Generator

Fixed-speed system

The system in the general sense implies the use of the squirrel cage induction generator, which provides the power output only through the stator winding. Figure 2 illustrates the configuration. It requires a grid-connected squirrel cage induction generator coupled to a turbine through a gear box. The gear steps up the rotor speed to a value matching a 50- or 60 Hz utility network. The generator always draws reactive power from the network. Capacitors are used to compensate this lagging VAR. These capacitors may cause the induction machine to self-excite, leading to over voltages at the time of the disconnection of the wind turbine from the electrical system if proper protective measures are not taken. Because of its coupling to the grid, the speed varies over a very small range above synchronous speed, usually around 1%. As the speed variation is small, the system is commonly known as a fixed-speed system. For such a system, the tip speed ratio varies over a wide range, making the rotor efficiency suffer at wind speeds other than the rated wind speed. The gear box ratio is selected for optimal C, for the most frequent wind speed. In a well-designed system, fixed-speed operation can extract about 80% of the energy available from a fully variable speed system over a year. Fixed-speed wind turbines employing either blade pitch regulation or stall regulation to limit the power at high wind speeds are used. It is necessary to do so because if the input mechanical power is more than the power corresponding to the pull-out torque, the system becomes unstable.

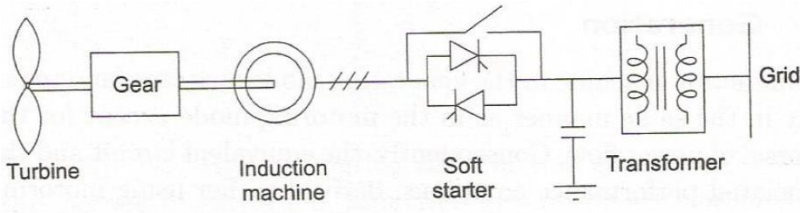

Fig. 2 Fixed-speed system with a squirrel cage induction generator

In a pitch-regulated system the electrical output power is regulated by a control system, which alters the blade pitch angle to extract the maximum energy at wind speeds below the rated wind speed; the power output is governed towards a limiting value at wind speeds above the rated speed. With stall regulation the blades are set at a constant pitch angle and the turbine enters the stall mode at high wind speed, thereby limiting the output power. Stall control is commonly applied in fixed-speed generators.

Appreciable generation at low wind speeds requires reduced rotor speed. To achieve this, one can use a two-speed cage-type induction generator with a stator winding arrangement for two different number of poles. The large number of poles is for low wind speed and the small number of poles is for high wind speed. An appropriately designed two-speed system can extract as high as 90% of the energy obtainable from a 100% variable-speed system over a year. With a two-speed system, the audible noise at lower wind speed is reduced.

Usually, the turbine accelerates the induction machine to syn chronous speed using wind power; the machine is then connected to the grid. The direct connection of an induction machine to the supply produces high inrush current, which is undesirable, partic ularly in the case of electrical networks with low fault tolerance levels. Such a connection can also cause torque pulsations, leading to gear box damage. In order to reduce the magnetizing current surge, soft-start circuits utilizing phase-controlled antiparallel thyristors (ac voltage controllers), as illustrated in Fig. 5.2, are frequently employed to control the applied stator voltage when the induction machine is connected to the network. A few seconds later, when normal current is established, these starting devices are bypassed. Such ac voltage controllers can also be used for connecting the machine to the grid during acceleration from zero speed to the operating speed. This is particularly useful in stall-controlled systems.

Semi-variable-speed operation

The advantages of a grid-connected, fixed-speed squirrel cage generator are its lower capital cost, simple system configuration, and robust mechanical design. As the rotor speed is nearly constant, fluctuations in wind speed result in torque (power) excursions, which may lead to unwanted grid voltage fluctuation and strains on the turbine components. Wind gusts in particular lead to large torque variations.

Limited variable-speed operation in this single-output system can bring down the pulsations in grid power (voltage) and me mechanical stress. If some of the generator shaft input (i.e., turbine output) can be dissipated in the rotor, the grid input power (which is essentially the power flow across the gap) can be levelled under fluctuating wind speed conditions. According to Eqns (3.11) and (3.40), the rotor electrical power is proportional to the slip. It then becomes possible to achieve speed control through control of the energy dissipated in a rotor resistor. Furthermore, the variation of rotor resistance with speed (i.e., with slip) in accordance with (R,+ R)/s constant [see Eqn (3.22)] keeps both the rotor current and the air-gap power torque multiplied by the synchronous speed) constant. Hence the main aim of the control strategy will be to keep the rotor current at a set value, irrespective of the speed variation within a range, for constant power output from the stator.

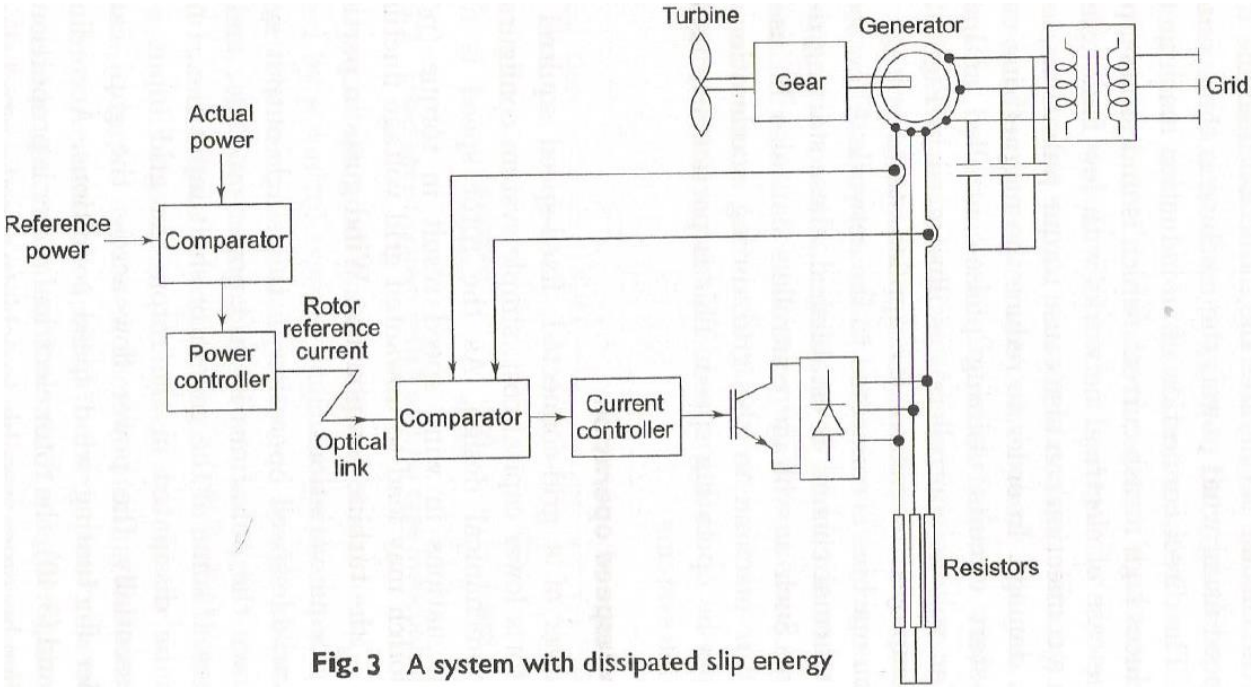

Fig. 3 A system with dissipated slip energy

Figure presents a configuration which includes a gear box, an induction motor with a three-phase stator winding, and a wound rotor with an electronically variable rotor resistance. The converter and the resistance rotate with the rotor. Control signals are sent to the rotating electronic parts by opto-electronic means. The rotor current reference comes from the comparison between the actual power and the reference power. The average resistance is varied between zero and the full value by continuously adjusting the duty cycle of the transistor switch. When the wind speed goes above the nominal value, the rotor current is held constant at a value corresponding to the rated power, by decreasing the duty cycle of the transistor switch. This will cause the generator speed to change, at the same time maintaining constant stator power. This configuration allows limited speed variation. The system shown in this figure is being marketed by Vestas of Denmark under the trade name OptiSlip with a maximum variation of 10% over nominal speed.

4.2.2 Doubly fed Induction generators

With a slip-ring induction machine, power can be fed into the supply system over a wide speed range by appropriately controlling the rotor power from a variable-frequency source. The provision for bidirectional flow of power through the rotor circuit can be achieved by the use of a slip-ring induction motor with an ac/dc/ac converter connected between the slip-ring terminals and the utility grid. The basic configuration of the system is shown in Fig. 4.The system is known as a double-output induction generator (DOIG) because power can be tapped both from the stator and from the rotor. Figure 5 presents the main components of the solid-state system for the controlled flow of slip power at variable speed through current converters. The intermediate smoothing reactor is needed to maintain current continuity and reduce ripples in the link circuit. For the transfer of electrical power from the rotor circuit to the supply, converters I and II are operated, respectively, in the rectification and inversion modes. On the other hand, for power flow in the reverse direction, converter II acts as a rectifier and converter I as an inverter. The step-down transformer between converter II and the supply extends the control range of the firing delay angle a2 of converter II.

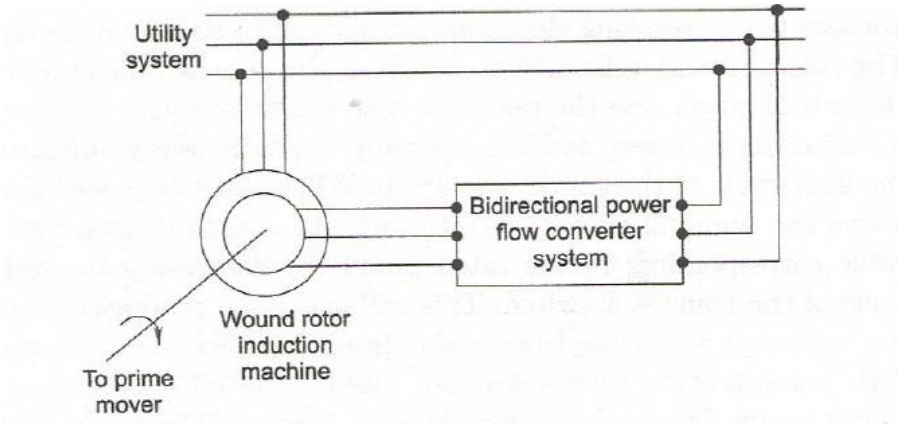

Fig. 4 Double-output induction generator system

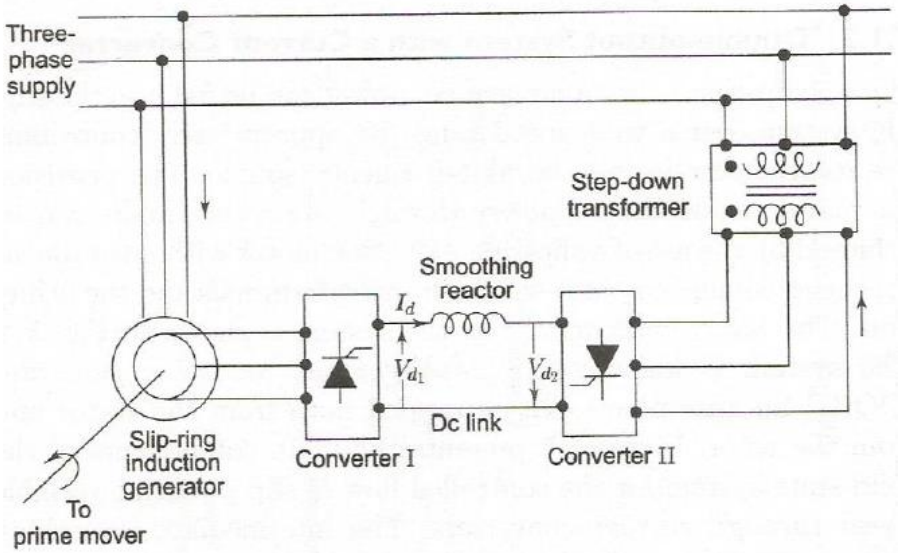

Fig. 5 Double-output system with direct current link

The firing delay angle a of converter I on the rotor side controls the phase difference between the injected rotor phase voltage and the rotor current, while the delay angle az of converter II on the line side dictates the injected voltage into the rotor circuit.

Line-commutated converters cannot generate leading VAR, and so, for maximization of the power output, a should be set at 0° (rectification mode) in the super synchronous region above the rated speed n, (see Fig. 3.5) to draw power out of the rotor, and at 180° (inversion mode) in the sub synchronous region to inject power at the slip frequency into the rotor circuit. Power flow characteristics can be studied using ac as well as dc equivalent circuits. A reasonable estimate for the required variation in a2 as a function of slip can be obtained by considering the de voltage balance between the two sides of the smoothing reactor in the anti parallel bridge network.

To derive the equivalent circuits and analyse this system, we make the following assumptions.

(a) The magnetizing current and iron loss are neglected.
(b) The inverter-side transformer is assumed to be ideal.
(c) The commutation of the switching devices is assumed to be instantaneous and the device losses are neglected.
(d) The harmonic effects are ignored.

4.3 Equivalent circuits

4.3.1 The ac equivalent circuit

Neglecting stator and rotor leakage impedance drop, the average voltage output of converter I at a slip s is given by

$$V_{d_1} = \frac{3}{\pi}\sqrt{6}V_2|s|\cos\alpha_1$$

where V is the slip-ring voltage (per phase) at standstill. For converter II, the average voltage output is given by

$$V_{d_2} = \frac{3}{\pi}\sqrt{6}\frac{V_1}{m_2}\cos\alpha_2$$

m_2 being the turn ratio of the step-down transformer between converter II and the supply.
For dc voltage balance, neglecting the resistance drop in the dc-link smoothing inductor

$$V_{d1} + V_{d2} = 0$$

This yields

$$\cos\alpha_2 = -\frac{m_2}{m_1}|s|\frac{V_2'}{V_1}\cos\alpha_1$$

where V_2' is the stator-referred, slip-ring open-circuit voltage. Equation (5.4) can be used for the evaluation of α_2. Under the assumption of negligible stator impedance drops, V_2' Equals V_1 and Eqn (5.4) becomes

$$\cos\alpha_2 = -\frac{m_2}{m_1}|s|\cos\alpha_1$$

In fact, the presence of the dc-link circuit resistance demands

$$\cos\alpha_2 \geq -\frac{m_2}{m_1}|s|\cos\alpha_1 \qquad (5.6)$$

Neglecting the losses in the semiconductor switches, the slip power, i.e., the rotor electrical power, is partly dissipated in the dc-link and rotor resistances, and the rest is fed back to the supply system through converter II. With reference to Fig. 5.5, the power input to converter II from the dc-link side (inverter operation) is

$$P_2 = -V_{d2}.I_d \qquad (5.7)$$

Using Eqn (5.2) in Eqn (5.7), we get

$$P_2 = -\frac{3}{\pi}\sqrt{6}\frac{V_1}{m_2}I_d\cos\alpha_2 \qquad (5.8)$$

For 120° conduction of each device in the converters, the fundamental rms component I_2 of the ac-side current of the converters (rotor or transformer secondary) and the dc-link current are related by

$$I_2 = \frac{\sqrt{6}}{\pi}I_d \qquad (5.9)$$

From Eqns (5.8) and (5.9), the power fed back to the supply by the rotor is obtained as

$$P_2 = -3\frac{V_1}{m_2}I_2\cos\alpha_2 \qquad (5.10)$$

Referring the current I, to the stator side, we get

$$P_2 = 3\frac{m_1}{m_2}V_1I_2'\cos\phi_2 \qquad (5.11)$$

where ϕ_2 is the supplementary of the delay angle α_2 of converter II (i.e., $\phi_2 = \pi - \alpha_2$).
The rms value of the quasi-square wave rotor current is

$$I_r = \sqrt{\frac{2}{3}}I_d \qquad (5.12)$$

The total secondary circuit copper loss

$$\begin{aligned} P_{Cu2} &= 3I_r^2R_r + I_d^2R_d \\ &= 3I_r^2(R_r + 0.5R_d) \end{aligned} \qquad (5.13)$$

The rotor rms current consists of the fundamental rms component and the higher harmonic rms components. Assuming that the torque is produced by the fundamental component of the rotor current, mechanical power can be expressed as

$$P_m = (\text{rotor-side electrical power with } I_2) \times \frac{1-s}{s}$$
$$= (P_{\text{Cu2}} \text{ due to } I_2 + P_2)\frac{1-s}{s}$$
$$= 3\left[I_2^2\,(R_r + 0.5R_d) + \frac{V_1}{m_2} I_2 \cos\phi_2\right]\frac{1-s}{s} \qquad (5.14)$$

The air-gap power is

$$P_{\text{ag}} = P_2 + P_{\text{Cu2}} + P_m \qquad (5.15)$$

Substituting the expressions for P2, PCw2, and Pm from Equations (5.11), (5.13), and (5.14), using Equations (5.9) and (5.12), and referring all the quantities to the stator side, we get

$$P_{\text{ag}} = 3\left[R'_x I'^2_2 + \frac{R'_B}{s} I'^2_2 + \frac{m_1}{m_2}\frac{V_1}{s} I'_2 \cos\phi_2\right] \qquad (5.16)$$

Where

$$R'_x = \left(\frac{\pi^2}{9} - 1\right)(R'_r + 0.5R'_d)$$
$$R'_B = (R'_r + 0.5R'_d)$$

Based on Eqn (5.16), we can draw a complete per-phase equivalent circuit, which includes the stator resistance and leakage reactance, as shown in Fig. 5.6. Now, the stator input power is given by

$$P_1 = 3I_1^2 R_s + P_{\text{ag}} \qquad (5.17)$$

With reference to Fig. 5.5 and following the motoring convention, the net electrical power output for the generating operation,

$$P_o = -(P_1 - P_2) \qquad (5.18)$$

The use of Eqns (5.11), (5.16), and (5.17) in Eqn (5.18) gives

$$P_o = -3\left[I_1^2 R_s + I'^2_2 R'_x + \frac{I'^2_2 R'_B}{s} + \frac{1-s}{s}\frac{m_1}{m_2} V_1 I'_2 \cos\phi_2\right] \qquad (5.19)$$

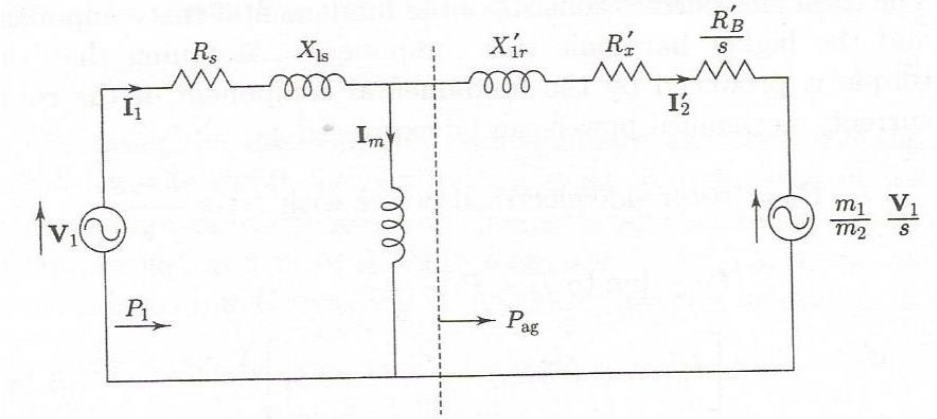

Fig. 5.6 Ac steady-state equivalent circuit per phase for the static Scherbius scheme

4.3.2 The dc equivalent circuit

In Fig. 5.7, the ac side (up to the rotor-side converter) represents the per-phase equivalent circuit of the induction machine referred to the rotor. The dc side of the equivalent circuit (to the right of the rotor-side converter) consists of the series resistance of the smoothing reactor and a voltage source representing the line-side converter.

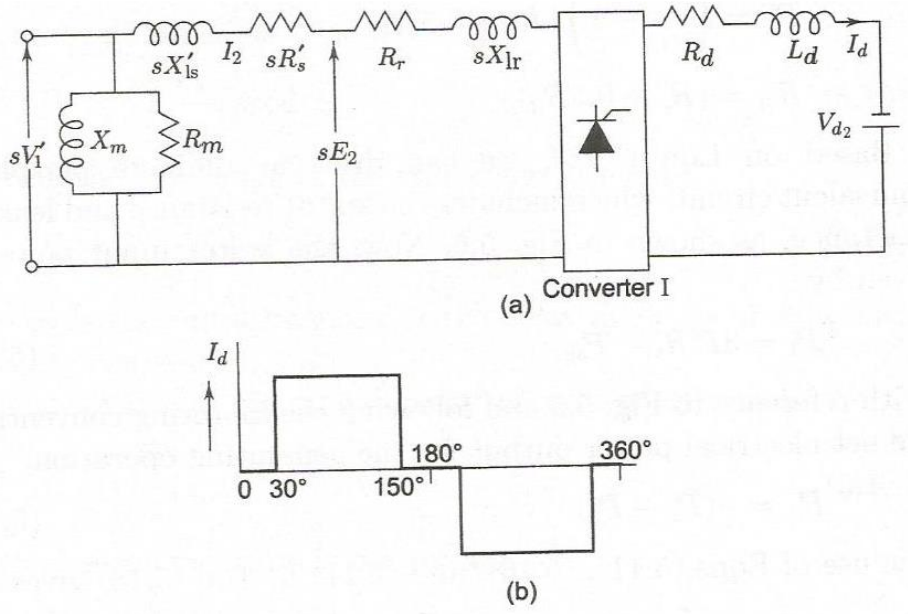

Fig. 5.7 (a) Rotor-referred induction motor equivalent circuit and dc link; (b) current waveform

It is convenient to refer the complete equivalent circuit to the de side. First the ac-side resistances sR_s', and R_r, are converted to their dc equivalents. To find out the dc equivalent resistance, recall that the input current of a phase-controlled converter has a quasi-square waveform as shown in Fig. 5.7(b). In this figure, the dc-side current is assumed to be ripple-free. The commutation overlap effect is also neglected. The rms value of the ac line current in terms of the dc current) is given by

$$I_r = \sqrt{\frac{2}{3}} I_d \qquad (5.20)$$

Now a resistance R connected to the dc side of the phase controlled converter I will be called the dc equivalent of the ac-side resistance if the power dissipated in Rde equals the total power dissipated in all three phases. The ohmic power dissipated in all the three phases of the induction motor is

$$p_{\text{Cu}} = 3I_r^2 (|s|R_s' + R_r) \qquad (5.21)$$

Using Eqn (5.20) in Eqn (5.21) gives

$$p_{\text{Cu}} = 2I_d^2 (|s|R_s' + R_r) \qquad (5.22)$$

Therefore, the equivalent de resistance of the induction motor when viewed from the dc-link side of converter I is

$$R_{\text{dc}} = 2|s|R_s' + 2R_r \qquad (5.23)$$

Once the resistance portion of the ac side equivalent circuit is transferred to the dc side, the rest of the ac circuit along with the rotor-side converter (I) can be represented by a de voltage source Vd, in series with an equivalent internal resistance Rd. This takes into account the reduction in the mean output voltage of converter I caused by the induction motor reactance. The values of Va and Rd, in terms of the ac-side circuit parameters are given by

$$V_{d_1} = \frac{3\sqrt{6}}{m_1 \pi} |s| V_1 \cos \alpha_1 \qquad (5.24)$$

and

$$R_{d_1} = \frac{3|s|}{\pi} (X_{\text{ls}}' + X_{\text{lr}}) \qquad (5.25)$$

Being an inductive phenomenon, R_{d1} does not represent a power loss component. Figure 5.8 shows the complete equivalent circuit referred to the de side. Note that the entire slip power, i.e., the rotor-side electrical power, is supplied to the right of the dotted line. From the figure,

$$I_d = \frac{V_{d_1} + V_{d_2}}{R_d + R_{d_1} + 2(|s|R_s' + R_r)} \quad \text{for} \quad I_d \geq 0 \qquad (5.26)$$

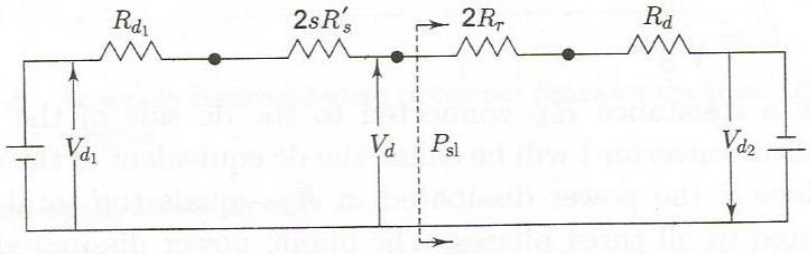

Fig. 5.8 The dc equivalent circuit referred to the rotor side

The condition $I_d \geq 0$ is required because the rotor-side and the line-side converter allow only unidirectional current. Substituting the expressions for V_{d1}, V_{d2} and R_{d1}, in Eqn (5.26) and arranging the terms, we get

$$I_d = \frac{3\sqrt{6}V_1\left(m_2|s|\cos\alpha_1 + m_1\cos\alpha_2\right)}{m_1 m_2[\pi(R_d + 2R_r) + |s|\left(2\pi R'_s + 3X'_{ls} + 3X_{lr}\right)]} \quad (5.27)$$

Since $I_d \geq 0$,

$$m_2|s|\cos\alpha_1 + m_1\cos\alpha_2 \geq 0 \quad (5.28)$$

The total electrical power in the rotor circuit, i.e., the slip power

$$P_{sl} = V_d I_d = (V_{d_1} - R_{d_1} I_d - 2|s|R'_s I_d) I_d \quad (5.29)$$

i.e.,

$$P_{sl} = |s|\left\{\frac{3\sqrt{6}V_1}{m_1\pi}\cos\alpha_1 - \left[\frac{3X'_{ls} + 3X_{lr}}{\pi} + 2R'_s\right] I_d\right\} I_d \quad (5.30)$$

As the slip power P_{sl} is s times the air-gap power,

$$P_{ag} = \text{sign}(s)\left\{\frac{3\sqrt{6}V_1}{m_1\pi}\cos\alpha_1 - \left[\frac{3X'_{ls} + 3X_{lr}}{\pi} + 2R'_s\right] I_d\right\} I_d \quad (5.31)$$

The approximate rms value of the fundamental component of the stator current for level dc-link current I_d is

$$I_1 = \frac{\sqrt{6}}{m_1\pi} I_d \quad (5.32)$$

Therefore, the stator input is

$$P_1 = P_{ag} + \frac{18R_s}{m_1^2\pi^2} I_d^2 \quad (5.33)$$

The power input to the utility grid through the supply-side converter (II) of the dc link is

$$P_2 = -V_{d_2} I_d = -\frac{3}{\pi}\sqrt{6}\frac{V_1}{m_2} I_d \cos\alpha_2 \quad (5.34)$$

As the motoring convention has been followed, the net electrical power output for the generating operation,

$$P_o = -(P_1 - P_2) = \left(P_{ag} + \frac{18I_d^2}{m_1^2\pi^2}R_s + \frac{3}{\pi}\sqrt{6}\frac{v_1}{m_2} I_d \cos\alpha_2\right) \quad (5.35)$$

4.4 Reactive power and harmonics

The grid-connected induction generator draws its excitation from the power line to set up its rotating magnetic field for regeneration and thus always demands lagging reactive power. Such

reactive power demand may adversely affect the network voltage level particularly in weak public utility networks-and increase system losses. For large wind turbines driving induction generators, the voltage fluctuation and the flickering arising from power output variation may exceed the statutory limits of the utility system.

By applying the definition of reactive power $Q = V_1 I_1 \sin\phi_1$, to the T-circuit model of an induction motor [shown in Fig. 3.3(a)] the reactive power in one phase of the motor under the approximation $I_1 \approx I_2'$ becomes

$$Q = X_m^2 I_m^2 + I_2'^2 (X_{ls} + X_{lr}') \quad (5.36)$$

The use of Eqn (5.9) in Eqn (5.36) yields

$$Q = X_m^2 I_m^2 + \frac{6}{\pi^2} \frac{I_d^2}{m_1^2} (X_{ls} + X_{lr}') \quad (5.37)$$

The reactive power consumed by the electrical machine thus comprises a constant value, which is the magnetizing volt-ampere, and a parabolic value dependent on the dc-link current. A three phase naturally commutated bridge converter on the rotor side is not capable of generating leading VAR. The lagging reactive power requirement is then transferred from the supply through the stator side of the machine, thus reducing the stator active power output for the same current loading. On the other hand, if the rotor-side converter is made a forced-commutated converter and its firing angle is made greater than 180° for operation below the rated speed and less than zero for operation above the rated speed, the reactive power demand of the machine can be met by the rotor-side converter. For controlled converter II, the phase angle between the fundamental alternating current and the ac sinusoidal current is equal to the firing delay angle α_2.

As α_2 is always less than 180°, the fundamental lagging reactive power requirement of converter II comes from the electrical source through the step-down transformer, and varies with the operating point. Here too, if forced commutation is employed, unity or leading power-factor operation in order to improve the overall power factor of the system is possible. Whatever may be the firing strategy, the current-fed dc-link converter system requires an expensive choke and an extra commutation circuit for operation at synchronous speed (if it lies within the operating speed range).

It also results in poor power factor at low-slip speeds. Besides, a current-fed de link generates rectangular current waves, which inject low-order harmonics into the supply side of converter II, which are difficult to eliminate. The low-order harmonics from converter I injected into the rotor mmf produce variable-frequency stator current harmonics and torque harmonics.

For the reactive power requirement of the supply-side converter, various compensation schemes can be applied. A PWM current inverter (converter II) may be used to feed the mains with a quasi sinusoidal current waveform with a phase shift, relative to the supply voltage, and can be controlled to generate reactive power.

The reactive power control range of a current-fed dc-link inverter is, however, very limited.

4.5 Double output system with VSI-Variable voltage, variable frequency generation

Following the motoring convention, if the slip is negative, the motor input current will lag behind the supply voltage by an angle greater than $\pi/2$, as shown in Fig. 5.14, implying the induction machine to be a source of power.

It is evident that the inverted motor current, i.e., the current flowing out of the machine, leads the motor terminal voltage.

The machine, therefore, acts as a source of active power feeding a parallel combination of a capacitor and a resistor as shown in Fig. 5.14(b). If the reactive power oscillation between the capacitor and the machine's effective inductance, similar to a parallel resonant circuit, can be maintained, a voltage will be sustained across the machine terminals. Initiation of the voltage build-up and its sustenance depend on several parameters, such as the load resistance, the capacitance, the speed, and the residual flux this is how a self-excited induction generator is obtained.

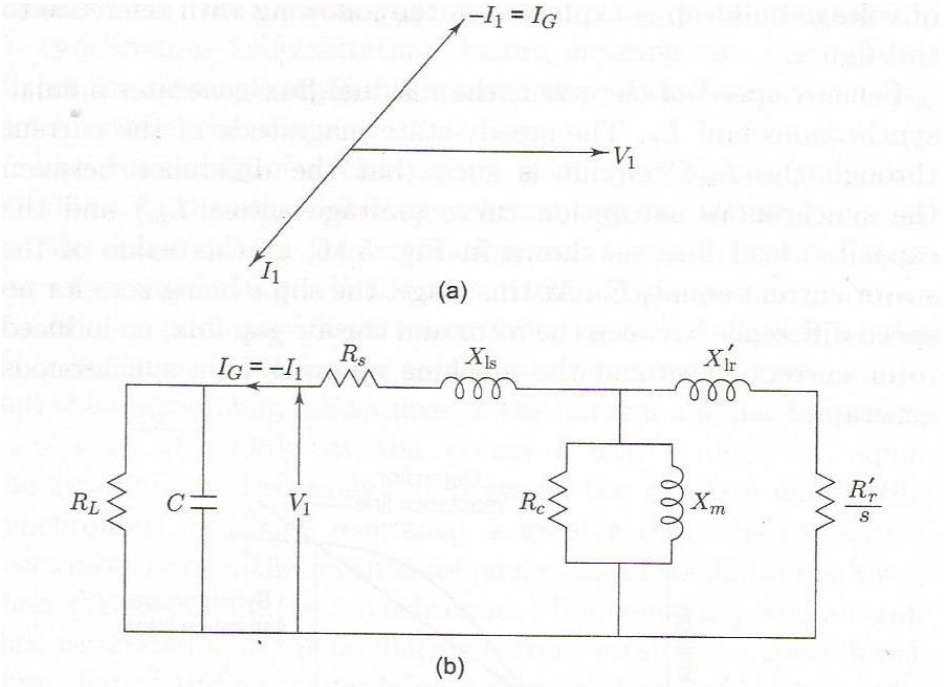

Fig. 5.14 Induction machine self-excitation: (a) phasor diagram, (b) basic equivalent circuit

4.5.1 Circuit Model

In contrast to the source-connected generator, the capacitor self excited induction generator presents a unique aspect-the main flux saturation assumes fundamental importance in establishing the equilibrium, that is, in determining the voltage level and the output frequency of the generator, for a given load, speed, and excitation capacitance. The capacitor is required to provide the reactive power, and no external constraints (frequency and/or flux) are imposed on the system. An uncontrolled self-excited induction generator shows considerable variation in its terminal voltage, degree of saturation, and output frequency under varying load conditions. For a systematic study of the behaviour of such a stand-alone induction generator with a variable-

frequency output, it is convenient to base the analysis on a circuit model whose parameters are defined in terms of a base frequency.

Figure 5.17 shows the per-phase, steady-state, stator-referred equivalent circuit of a self-excited induction generator connected to a resistive-inductive load. A capacitor of capacitance Co is connected to provide the excitation VAR.

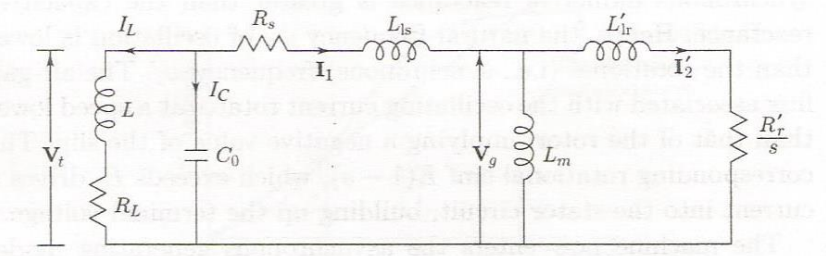

Fig. 5.17 Circuit model for a self-excited induction generator at stator frequency

With reference to Fig. 5.17, the following voltage equations in phasor notation can be written:

$$\mathbf{V}_t = R_s\mathbf{I}_1 + j\omega L_{ls}\mathbf{I}_1 + \mathbf{V}_g \tag{5.61}$$

which may be rewritten as

$$\mathbf{V}_t = R_s\mathbf{I}_1 + jFX_{ls}\mathbf{I}_1 + \mathbf{V}_g \tag{5.62}$$

where $F\ (= \omega/\omega_b)$ is the per-unit frequency and $X_{ls} = \omega_b L_{ls}$; w_b is the base angular frequency. Dividing Eqn (5.62) by F yields

$$\frac{\mathbf{V}_t}{F} = \frac{R_s}{F}\mathbf{I}_1 + jX_{ls}\mathbf{I}_1 + \frac{\mathbf{V}_g}{F} \tag{5.63}$$

The per-unit slip is

$$s = \frac{n - n_r}{n} \tag{5.64}$$

where n_r is the synchronous speed corresponding to the generated terminal frequency. The slip given in Eqn (5.64) may be expressed as

$$s = \frac{F - v}{F} \tag{5.65}$$

where v is the per-unit speed (n_r/n_b) defined with respect to the synchronous speed corresponding to the base frequency f_b and F is as defined earlier.

The voltage equation for the rotor circuit shown in Fig. 5.17 is

$$\mathbf{V}_g = \left(\frac{R'_r}{s}\right)\mathbf{I}'_2 + j\omega L'_{lr}\mathbf{I}'_2 \tag{5.66}$$

In terms of the parameters F and v, Eqn (5.66) becomes

$$\frac{\mathbf{V}_g}{F} = \frac{R'_r}{F-v}\mathbf{I}'_2 + jX'_{lr}\mathbf{I}'_2 \tag{5.67}$$

At the stator terminals, the following current balance equation holds:

$$-\mathbf{I}_1 = j\omega C_o \mathbf{V}_t + \frac{\mathbf{V}_t}{R_L + j\omega L}$$

In terms of the parameter F, this equation becomes

$$\mathbf{I}_1 = -\frac{\mathbf{V}_t}{F}\left[\frac{1}{(-jX_{cb}/F^2)} + \frac{1}{R_L/F + jX_{Lb}}\right] \tag{5.68}$$

where X_{cb} (= $1/w_bC_o$) and X_{Lb} (=w_bL) are, respectively, the reactance's of the excitation capacitor and the inductor at the base frequency.

Equations (5.63), (5.67), and (5.68) redefine the parameters and the node voltages of the equivalent circuit shown in Fig. 5.17, as indicated in Fig. 5.18. This stator-referred equivalent circuit, mapped in terms of the base frequency, is commonly used for predicting the performance of a self-excited induction generator.

In general, the speed and the load are the given parameters. The frequency, the excitation capacitance, and the magnetizing reactance constitute the set of unknown variables even when a desired terminal voltage is required to be maintained.

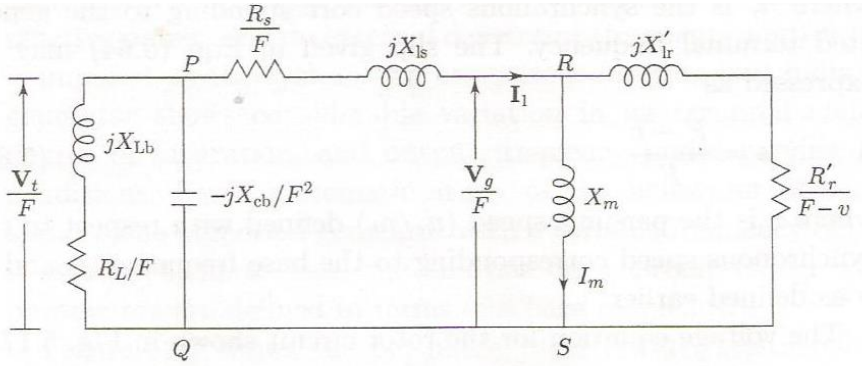

Fig. 5.18 The stator-referred circuit model of a self-excited induction generator normalized to the base frequency

4.5.2 Analysis of the Steady-state Operation

The equivalent circuit shown in Fig. 5.18 forms the basis for invest tigating the steady-state performance of a self-excited induction generator (SEIG) supplying a balanced load. There are two basic approaches, namely, the loop impedance method and the nodal admittance method, to defining the performance equations. The choice of the method is influenced by the objective of the analysis.

4.5.2.1 The loop impedance method

Since there is no emf source, applying Kirchhoff's emf law around the loop SRPQ in the circuit of Fig. 5.18 yields

$$(Z_{QP}+Z+PR+Z_{RS})/I_1 = 0 \qquad (5.69)$$

For the stator current to exist under the self-excited state, the sum of the impedances must be zero, i.e.,

$$Z_{QP} + Z_{PR} + Z_{RS} = 0 \qquad (5.70)$$

By equating the real and the imaginary parts independently to zero, we obtain two simultaneous non-linear equations:

$$f_1(F, X_{cb}, X_m) = 0$$
$$f_2(F, X_{cb}, X_m) = 0 \qquad (5.71)$$

Two equations can yield only two unknown variables. The key unknown variable in determining the performance an induction generator is the per-unit frequency F. The choice of the second unknown variable depends on the specific objective, i.e., the characterization of the problem. If the estimation of the minimum excitation capacitance for voltage build-up or the capacitance required for a specified value of the terminal voltage under a given load and speed is the requirement, X_{cb} is considered to be the unknown while X_m is given a specific value lying in the saturated region. The functions given by Eqn (5.71) then assume the forms

$$a_1F^3 - a_2F^2 - (a_3X_{cb} + a_4)F + a_5X_{cb} = 0 \qquad (5.72)$$

and

$$b_1F^4 - b_2F^3 - (b_3X_{cb} + b_4)F^2 + (b_5X_{cb} + b_6)F + X_{cb}b_7 = 0 \qquad (5.73)$$

where

$$\begin{aligned}
a_1 &= R_L TW + X_{Lb}T(R_s + R'_r) \\
a_2 &= vT(R_L W + R_s X_{Lb}) \\
a_3 &= R'_r(X_{Lb} + T) + T(R_s + R_L) \\
a_4 &= R_L R_s R'_r \\
a_5 &= vT(R_L + R_s) \\
b_1 &= X_{Lb}TW \\
b_2 &= vb_1 \\
b_3 &= T(X_{Lb} + W) \\
b_4 &= R_L T(R_s + R'_r) + R_s R'_r X_{Lb} \\
b_5 &= vb_3 \\
b_6 &= vR_L R_s T \\
b_7 &= R'_r(R_L + R_s)
\end{aligned} \qquad (5.74)$$

in which

$$T = X_{ls} + X_m$$
$$= X'_{lr} + X_m$$
$$W = X'_{lr} + X_{ls} || X_m$$

Equations 5.72 and 5.73 can be solved numerically to obtain the values of X_{cb} and F. The initial value of C should be well above the value required for self-excitation under load and F should be less than the per-unit speed, though close to it.

A mathematical model similar to Eqns (5.72) and (5.73), in terms of the unknown variables X_m and F, can be formulated from Eqn (5.71) for given values of the excitation capacitance, the load, and the speed.

Once the values of X_{cb} (or X_m) and F are obtained, the following circuit relations can be used to determine the generator performance. The magnetization characteristic gives the values of the air-gap voltage V_g/F and the magnetizing current I_m corresponding to the chosen (evaluated) value of X_m:

$$\mathbf{I}_1 = \mathbf{I}_m + \frac{\mathbf{V}_g/F}{R'_r/(F-v) + jX'_{lr}}$$
$$\mathbf{V}_t = \mathbf{V}_g + \mathbf{I}_1(R_s + jFX_{ls})$$
$$\mathbf{I}_L = \frac{\mathbf{V}_t}{R_L + jFX_{Lb}}$$

The output power is

$$P_o = 3|I_L|^2 R_L \qquad (5.75)$$

Using the mathematical model presented above, the performance of an SEIG over a wide range of speeds, load impedances, and capacitances can be predicted from the equivalent circuit parameters and the magnetization characteristic at the base frequency.

4.5.2.2 The nodal admittance method

The nodal admittance method has the advantage that it decouples the load and the excitation capacitor branch, and enables the per unit frequency to be determined independent of the value of X_{cb}.

Figure 5.18 can be redrawn as Fig. 5.19, where

$$R_{RS} = \frac{(F-v)R'_r X_m^2}{R_r^2 + (F-v)^2(X_m + X'_{lr})^2}$$
$$X_{RS} = \frac{R'^2_r X_m + (F-v)^2 X_m X'_{lr}(X_m + X'_{lr})}{R_r^2 + (F-v)^2(X_m + X'_{lr})^2}$$

The total impedance Z_{PS} of branch PRS is given by

$$Z_{PS} = \left(\frac{R_s}{F} + R_{RS}\right) + j(X_{\text{ls}} + X_{RS})$$

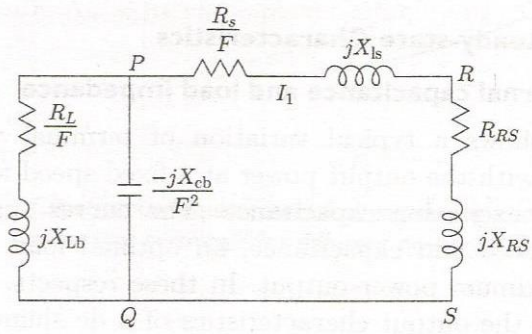

Fig. 5.19 The simplified equivalent circuit of a self-excited induction generator

By applying Kirchhoff's current law in Fig. 5.19, the sum of the current at node P equals zero:

$$(Y_L + Y_C + Y_{PS})V_P = 0 \tag{5.76}$$

where YL, Yc, and Yp are, respectively, the admittances of the series load circuit, the capacitive excitation circuit, and the machine equivalent circuit. Since Vp cannot be zero, for successful voltage build-up, it follows that

$$Y_L + Y_C + Y_{PS} = 0 \tag{5.77}$$

Equating the real and the imaginary parts independently to zero, the following equations are obtained:

$$\frac{R_L F}{R_L^2 + F^2 X_{\text{Lb}}^2} + \frac{F R_s + F^2 R_{RS}}{(R_s + F R_{RS})^2 + F^2 (X_{\text{ls}} + X_{\text{RS}})^2} = 0 \tag{5.78}$$

$$\frac{F^2}{X_{\text{cb}}} - \frac{F^2 X_{\text{Lb}}}{R_L^2 + F^2 X_{\text{Lb}}^2} - \frac{F^2 (X_{\text{ls}} + X_{\text{RS}})}{(R_s + F R_{RS})^2 + F^2 (X_{\text{ls}} + X_{RS})^2} = 0 \tag{5.79}$$

Equations (5.78) and (5.79) are alternatives to Eqns (5.72) and (5.73), and are thus amenable to solution in the same manner.

One marked difference can be noted: Eqn (5.78) is independent of X_{cb} and can be expressed as a 6th degree polynomial in F if the level of saturation, i.e., Xm, has been decided upon earlier. In certain studies, Eqns (5.78) and (5.79) are found to be more convenient.

4.5.3 The Steady-state Characteristics

4.5.3.1 Effect of external capacitance and load impedance

Figure 5.20 shows a typical variation of terminal voltage for resistive lead with the output power at a fixed speed for different values of the excitation capacitance. The curves suggest that, for a given speed and capacitance, an optimal load impedance exists for maximum power output. In these respects, the curves are similar to the output characteristics of a dc shunt generator with

different field circuit resistances. The frequency decreases with the lead, but this variation is not significantly affected by the capacitance. Figure 5.21 exhibits the manner in which the capacitance requirement changes with the load and the power factor for constant terminal voltage at a fixed speed. The figure also indicates an increase in the VAR demand with decreasing load power factor.

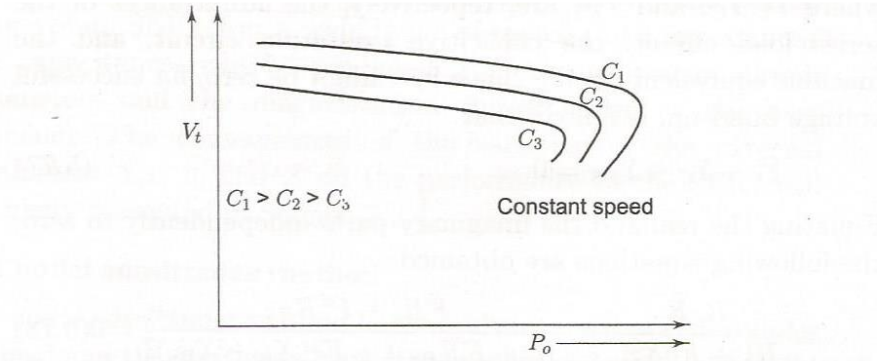

Fig. 5.20 Voltage regulation for different values of the excitation capacitance at constant speed

The group of curves shown in Fig. 5.22 shows the effect of controlling the excitation capacitance on the terminal voltage and the output power for a fixed load impedance at a constant speed.

As is clear from these figures, there exist optimal capacitances that maximize the output power and terminal voltage for a given load impedance at a fixed speed.

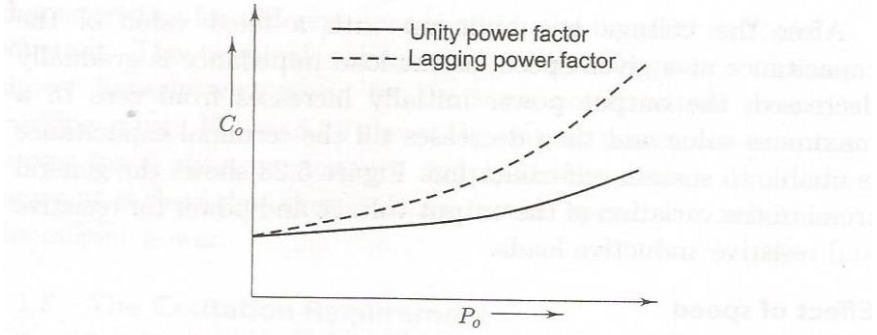

Fig. 5.21 Capacitance requirements for maintaining a constant voltage at the generator terminals for different power factors

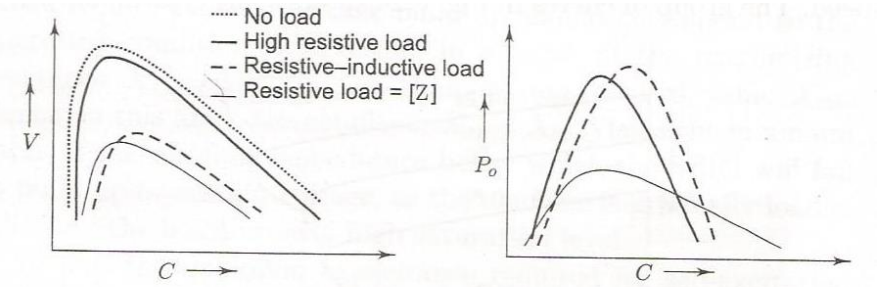

Fig. 5.22 Effect of the capacitance on the terminal voltage and the output power for a fixed load impedance

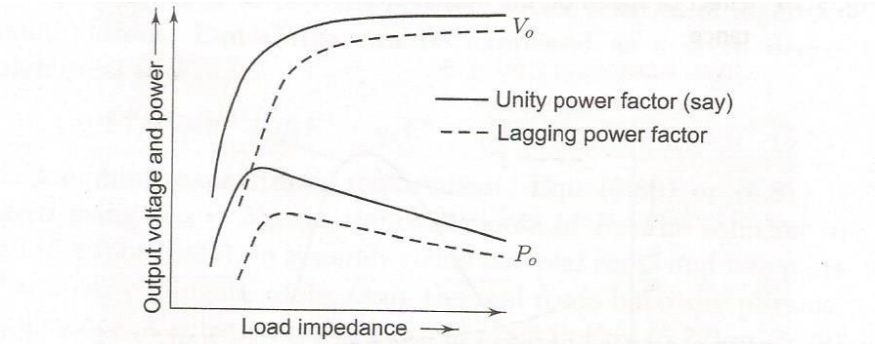

Fig. 5.23 Output voltage and power versus load impedance magnitude for different power factors at a fixed speed and constant capacitance

After the voltage has built up with a fixed value of the capacitance at a given speed, as the load impedance is gradually decreased, the output power initially increases from zero to a maximum value and then decreases till the terminal capacitance is unable to sustain self-excitation. Figure 5.23 shows the general trend in the variation of the output voltage and power for resistive and resistive-inductive loads.

4.5.3.2 Effect of speed

For power generation using wind energy, the speed of the prime mover varies over a wide range. For self-excitation, as indicated by the capacitive reactance value Xc/F, the capacitor size is approximately proportional to the inverse of the square of the speed. The group of curves in Fig. 5.24 shows some typical output characteristics for different speeds under the constraint Xcb/v2 = constant.

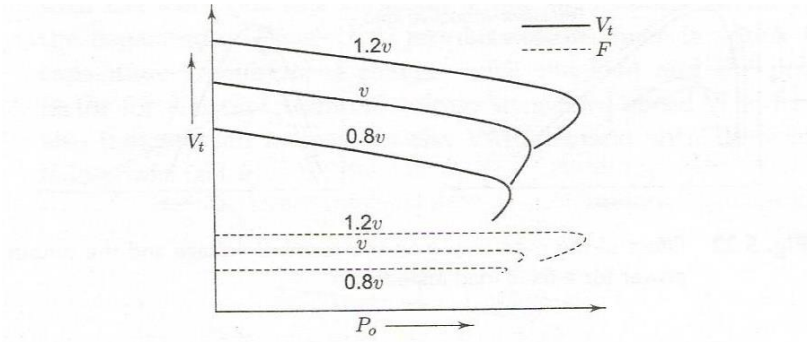

Fig. 5.24 Effect of speed on the output characteristics for constant capacitance

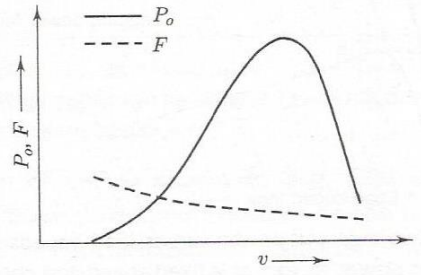

Fig. 5.25 Output power and frequency variation with speed

The terminal voltage and output frequency increase almost linearly with speed for the same power output over the working range. Figure 5.25 shows the output power versus speed curves for a given capacitance and load impedances. From the figure, it is clear that there exists a certain speed that maximizes the output power.

4.6 Effect of wind generator on the network

Many wind farms are connected to the local network at low, medium, or high voltage. The injection of wind power into the network has an impact on the voltage magnitude, its flicker, and its waveform at the point of common coupling (PCC).

The effect on the voltage magnitude depends on the strength of the utility distribution network at the point of coupling as well as on the active and reactive power of the wind generator(s).

The strength of the system at the point of coupling under consideration is decided by the short-circuit power, called the fault level, at that point. The short-circuit power is the product of the short-circuit current, following a three-phase fault at that point, and the voltage of the system. In fact, a power system comprises many interconnected power sources. The loads are fed through extended transmission and distribution networks. At the point of connection, as illustrated in Fig. 5.28(a), an equivalent ideal voltage source in series with an impedance Z, may be assumed to replace the power system. Thus, the higher the fault current, the lower the source impedance. The wind farm with induction generators receives reactive power from the network and delivers real power to it. Without contribution from the wind generator, the fault level at the point of connection near the wind farm is

$$M = I_f V_s \tag{5.90}$$

where

$$I_f = V_s / Z_s$$

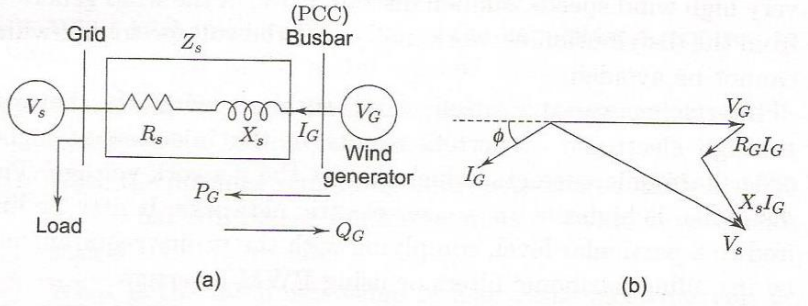

Fig. 5.28 (a) Schematic diagram of generator connection and distribution; (b) phasor diagram

Thus the fault level and hence the network strength are indicative of the source impedance. Areas of high wind velocity are suitable locations for wind farms. These areas are usually sparsely populated. Long transmission and distribution lines are normally required for connecting wind

farms with the power system network. As a result, fault level at the wind farms are generally low, making them weak electrical systems.

With reference to Fig. 5.28(b), if the phase difference between V_s and V_G is not large, the voltage at the PCC will be close to

$$V_G = V_s + R_s I_G \cos\phi - X_s I_G \sin\phi$$
$$= V_s + \frac{P_G R_s}{V_G} - \frac{Q_G X_s}{V_G} \quad (5.91)$$

Thus, at low power delivery, the voltage at the PCC reduces if the induction generator absorbs reactive power from the grid, while, at increased power flow, the voltage rises. Flicker is defined as the unsteadiness of the distribution network voltage. It may be caused by the continuous operation of a wind turbine or the switching operations of turbines. While operating, the rotor of a wind turbine experiences a cyclic torque variation at the frequency with which the blades move past the tower. This cyclic power variation may lead to flicker, and depends on the wind speed distribution at the site. While being connected to the network, the induction generator draws excessive current. Soft-start systems are usually employed to minimize the transient inrush current. However, at very high wind speeds, sudden disconnection of the wind generator from the distribution network may cause the voltage to dip, which cannot be avoided.

Interfacing variable-speed wind turbines with the network through electronic converters results in the injection of higher order harmonic currents, which distort the network voltage. This distortion is higher with weaker electric networks. It may be lim ited to a particular level, complying with the utility requirements, by installing harmonic filters or using PWM inverters.

4.7 Wind speed measurements

The device used for wind speed measurement is called an anemometer. There are three different techniques for wind speed measurement. In general, any measurable phenomenon that has strong dependence on wind velocity can be used for wind speed measurement. Experience has shown that thrust, pressure, and the cooling effect, are the three most convenient parameters using which wind speed can be directly measured.

4.7.1 Robinson Cup Anemometer

The Robinson cup anemometer consists of a vertical shaft carrying three or four horizontal arms, at the ends of which there are hemispherical cups of thin sheet metal. The circular rims of the cups are in vertical planes passing through the common axis of rotation. The thrust of wind is greater on the concave sides than on the convex ones, thereby leading to the rotation of the vertical shaft (Fig. 2.1).

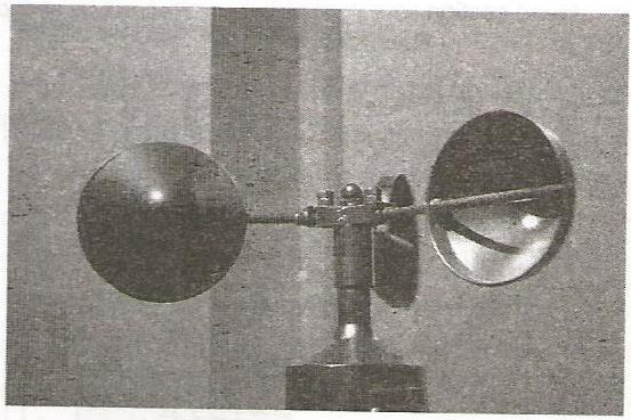

Fig. 2.1 The Robinson cup anemometer

As this is a vertical-axis device, there is no problem of orientation along the wind direction. The wind velocity has a linear relationship with the speed of rotation, which is measured by a photocell operated digital counter. The display can be precalibrated to give the wind speed directly. Modern devices have facilities for continuous data logging and storage, from which data can be retrieved later for analysis.

At very low wind speeds, the readings of the cup anemometer can be erroneous due to the friction of the bearings. During fast variations of wind speed, the inertia effect may be significant;

e.g., when the wind speed drops quickly, the anemometer tends to rotate faster and takes time to slow down. In spite of these minor drawbacks, the Robinson cup anemometer is the most extensively used instrument for wind speed measurement.

4.7.2 Pressure Tube Anemometer

The pressure tube anemometer a simple mechanical device suitable for stand-alone application in remote windy locations. Structure-wise, it has two distinct parts. The head, which is usually mounted on a mast at the desired height, consists of a horizontal tube, bent at one end and supported by two concentric vertical tubes. The horizontal end is connected to the inner tube.

At the other side of the outer tube, there are a few holes a little below the horizontal tube. The entire head is free to rotate, which is turned to face the wind by a vane.

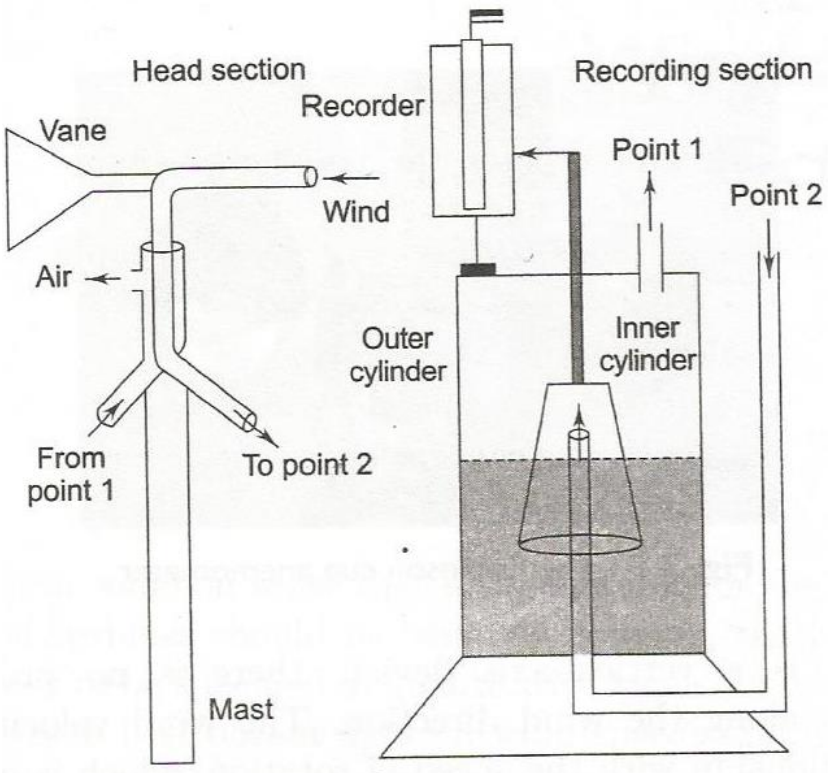

Fig. 2.2 The pressure tube anemometer

The wind blowing into the horizontal tube creates pressure, which is communicated through a flexible tube to a recorder.

Again, the wind blowing over the small holes in the concentric tube creates a suction effect, which is also communicated to the recorder through a second flexible tube.

In the recording apparatus, a copper vessel, closed at one end, floats inverted in a cylindrical metal container partly filled with water and sealed from the outside air. The wind pressure from the horizontal tube of the head is transmitted to the space inside the float, causing it to rise as wind blows. This is assisted by the suction that is applied to the space above the float.

Thus, as the wind speed rises and falls, the float also rises and falls, and its motion is transferred to a pen tracing a record on a sheet of paper by means of a rod passing through an airtight passage at the top of the cylinder. If the paper movement is spring operated, the device does not need any electrical supply.

The float can be so shaped, in accordance with the law relating pressure to wind velocity, that the velocity scale on the chart is linear. Most pressure tube anemometers also have wind direction recorders taking signals from the tail-vane, so that both the speed and direction of wind are recorded.

4.7.3 Hot Wire Anemometer

A hot wire anemometer uses the cooling effect of wind on an electrically heated platinum or tungsten wire to measure wind velocities. The wire is heated by a constant-current source. With the variation of wind speed, the wire temperature varies, which varies the resistance of the wire. Naturally, in order to find the wind speed, it suffices to measure the resistance of the wire using any standard method. The calibration has to take into account the resistance-temperature characteristics of the wire and the ambient temperature of air.

In a hot wire anemometer, the temperature difference between the wire and the ambient air is inversely proportional to the square root of the wind velocity:

$$T_w - T_a \propto \frac{1}{\sqrt{v}} \tag{2.1}$$

Because of this relation, this anemometer is useful especially for measuring small wind velocities.

4.8 Wind speed statistics

Since the power contained in wind varies with the cube of the wind speed, the average wind speed available at a particular site is the first criterion to be considered in site selection. During the site identification process, the measuring instruments described in the previous section are installed at the site. The annual average wind speed is calculated according to the equation

$$\overline{v} = \frac{1}{t_2 - t_1} \int_{t_1}^{t_2} v \, dt \tag{2.2}$$

where $\overline{v}$ is the annual average wind speed (m/s), v is the instantaneous wind speed (m/s), and $t_2 - t_1$ is the duration of one year (8760 hrs).

In the case of a digital data logger recording wind speed data at regular intervals, the average wind speed can be calculated as

$$\overline{v} = \frac{1}{n} \sum_{i=1}^{n} v_i$$

where v_i is the wind speed at the ith observation and n is the number of observations.

At any given site, the wind speed varies with the height from the ground level. It is generally not possible to install measuring instruments at all heights, but an empirical formula can be used to find the mean wind speed at a certain height using the observed mean wind speed at 10 m:

$$\overline{v}_H = \overline{v}_{10} \left(\frac{H}{10} \right)^x \tag{2.3}$$

where $\overline{v}_H$ is the annual average wind speed at height H (m/s), $\overline{v}_{10}$ is the annual average wind speed at 10 m (m/s), and x is an exponent that depends on the roughness of the ground. The values of x are given in Table 2.1.

Table 2.1 Values of the boundary layer exponent x for varying ground roughness

Description of land	Exponent x
Smooth land with very few obstacles (e.g., sea, coast, desert, snow)	0.10–0.13
Moderately rough, (e.g., agricultural fields with very few trees, grasslands, rural areas)	0.13–0.20
Land with uniformly distributed obstacles 10–15 m high (e.g., forests, small towns, agricultural fields with tree plantations)	0.20–0.28
Land with big and non-uniform obstacles (e.g., big cities, plateaus)	0.28–0.40

The measuring instruments record the wind speed continuously against time. If the data are collected throughout a year, the resulting chart would look like a long wavy line, as shown in Fig. 2.3.

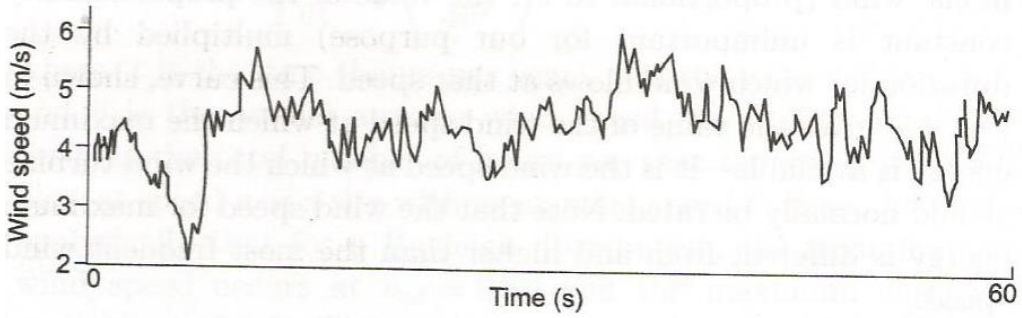

Fig. 2.3 Typical anemometer recording of wind speed versus time

It is clear that this plot is too wavy and irregular for us to obtain any useful information from it. The next step is to obtain, from Fig. 2.3, the plot of wind speed v versus the total time during a year for which the wind speed is v (Fig. 2.4), called the wind speed distribution curve. Of course, the period of time for which the wind speed assumes an exact value is infinitely small. So, the vertical axis actually gives the annual duration for which the wind speed falls within certain limits, for instance 0.5 m/s below and above v. The y-axis of the wind speed distribution curve should be given in hours per annum per meter per second. Thus the integral of the function (or the area under the curve) will always be 8760 hrs, corresponding to the number of hours in a year.

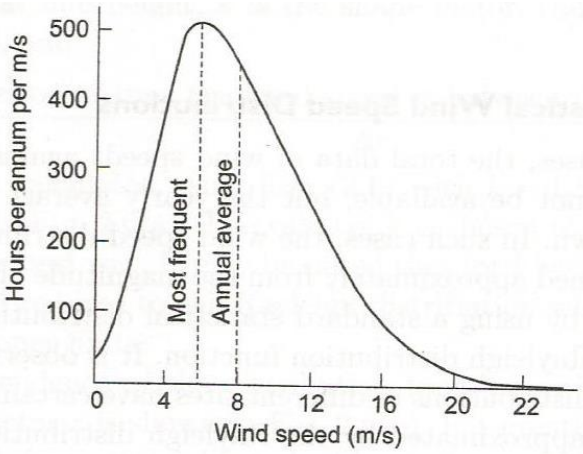

Fig. 2.4 Plot with wind speed on the x-axis and the duration in a year for which wind assumes that speed on the y-axis

It is easy to plot the energy distribution curve for a site the energy available at a particular wind speed is the power contained in the wind (proportional to v, the value of the proportionality constant is unimportant for our purpose) multiplied by the duration for which wind blows at that speed. This curve, shown in Fig. 2.5, gives the value of the wind speed at which the maximum energy is available it is the wind speed at which the wind turbine should normally be rated. Note that the wind speed for maximum energy is different from and higher than the most frequent wind speed.

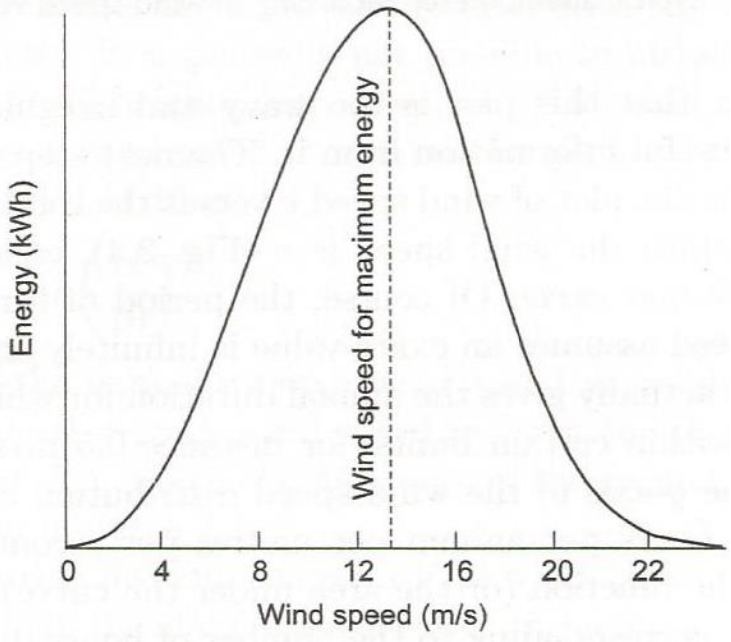

Fig. 2.5 The energy distribution curve

4.9 Site and turbine selection.

Site selection involves not only the choice of the geographical location for a wind turbine or a wind farm, but also the model of the turbine that is best suited to a particular site.

For the final selection process, that is, while choosing the wind turbine that is best suited for a particular site, a modification of the curve shown in Fig. 2.4 is necessary. At this stage, we plot the speed-duration curve the graph of v versus the total duration for which the wind speed exceeds or equals v (Fig. 2.7). Naturally, the largest coordinate on the y-axis is the number of hours in a year (8760), when the wind speed exceeds zero. If the wind speed is measured using a digital recorder with data logging facility, the wind speed distribution and duration curves can be obtained directly or generated by a computer later using the stored data.

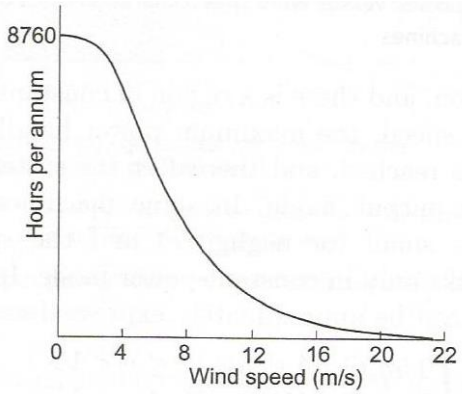

Fig. 2.7 The wind speed–duration curve: plot with wind speed along the x-axis and the duration for which the wind speed equals or exceeds that speed along the y-axis

The productivity of any wind generator at a particular site depends on the characteristics of the site (given by Fig. 2.7) and those of the wind machine. The latter are given as the power versus wind speed characteristics (such as that shown in Fig. 2.8), which are generally available for all commercially produced wind machines.

Every wind turbine model has a specific cut-in speed, a rated speed, a furling speed, and power versus wind speed characteristics within the wind speed range between the cut-in speed and the furling speed. At the cut-in speed the wind generator starts generating power. As the wind speed increases, the power output increases in proportion with the power contained in the wind. After the rated speed is reached, the speed-regulating mechanism comes into action, and there is a region of constant speed.

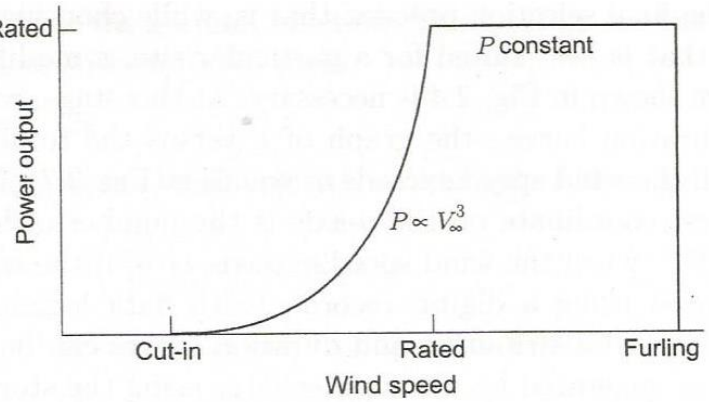

Fig. 2.8 Typical power versus wind speed characteristics of constant-speed wind machines

Beyond a certain wind speed, the maximum power handling capacity of the generator is reached, and thereafter the system works in the constant-power output mode. In some machines the constant speed region is small (or negligible) and the speed-regulating mechanism works only in constant-power mode. In such cases the characteristics can be approximately expressed as

$$P(v) \approx \begin{cases} 0.5\eta_v C_p \rho A v^3 \text{ for } V_c \le v < V_r \\ 0.5\eta_v C_p \rho A V_r^3 \text{ for } V_r \le v < V_f \end{cases} \quad (2.18)$$

where V_c is the cut-in speed, V_r is the rated speed, V_f is the furling speed, η_v is the efficiency of generator and mechanical transmission, C_p is the wind turbine coefficient of performance, ρ is the density of air, A is the blade swept area, and v is the wind speed. At the furling wind speed, the plant is shut down to avoid damage.

From Fig 2.8 and 2.7, the wind generator's characteristics, as weighted by the site's wind speed-duration curve, yield the power-duration characteristics. For each value of wind speed shown in Fig. 2.7, the corresponding value of the output power is obtained from Fig. 2.8. The typical output power-duration curve for a wind turbine is shown in Fig. 2.9. To illustrate, we have also shown the wind power-duration curve (obtained by the relation $0.5\eta_v C_p \rho A v^3$), so that the energy loss due to cut-in and furling becomes clear.

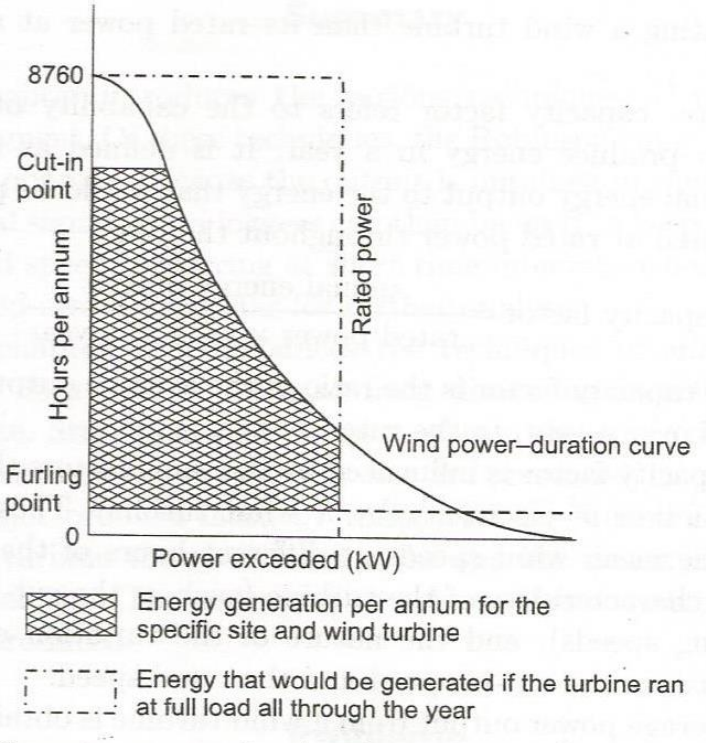

Fig. 2.9 The output power–duration characteristics of a wind generator at a given site

The area under the output power-duration curve measures the energy output of a particular machine at a given site. By plotting similar curves for different machines is at a particular site, one can choose the appropriate machine. One generally chooses the model that gives the maximum output for a specific rated power at a particular site.